

STOCHASTIC MODEL OF MULTIPLE CRACKING PROCESS IN FIBER REINFORCED CEMENTITIOUS COMPOSITES

P. Kabele and M. Stemberk

Czech Technical University in Prague, Faculty of Civil Engineering, Czech Republic

ABSTRACT

An analytical model that allows prediction or reproduction of the overall stress-strain relationship of a high performance cementitious composite in tension is presented. Through consideration of stochastic character of the composite microstructure, the model captures the sequence of crack formation and the load fluctuations that are characteristic for the process of multiple cracking. The proposed model is used to reproduce/predict hardening stress-strain curves of an Engineered Cementitious Composite (ECC). Results capture the effect of introducing artificial flaws on the composite ductility, which has been reported in experimental studies.

1 INTRODUCTION

Multiple cracking is a fracture phenomenon observed in certain fiber-reinforced brittle-matrix composites when they are exposed to tensile stress. As opposed to formation of a single localized crack, multiple cracking manifests itself by generation of a large number of distributed matrix cracks bridged by fibers. These cracks usually form a very fine pattern, having spacing much smaller than length and exhibiting very small (sub-millimeter) opening displacements (see inset in Figure 1). Consequently, multiple cracking permits the composite material to accommodate significant deformations while retaining a macroscopic integrity and small crack width. Composites with cement-based matrix exhibiting such a behavior are often desirable in the field of civil engineering; namely as materials for repair of reinforced concrete structures, durable bridge deck overlays, continuous pavements, anti-seismic retrofit and others.

Over the past decade, a micromechanics- and fracture mechanics-based methodology has been developed, which facilitates a conscious design of cement-based material composition so as to achieve multiple cracking even with low volume fractions of short random fibers. Due to low fiber content, these materials can be easily mixed and shaped by various techniques (casting, extrusion, spraying, etc.). Composites produced according to the latter methodology are called Engineered Cementitious Composites (ECC) (Li [1]).

In the ECC material design theory, the effect of fibers spanning a matrix crack (fiber bridging) is accounted for through the relationship between bridging stress and crack opening displacement. Then, in order to achieve multiple cracking the following two criteria have to be simultaneously satisfied (Leung [2]):

- (a) The ‘*steady state cracking criterion*’ requires that a matrix crack can eventually grow under constant applied far field uniaxial tensile stress, as the bridging stress in the middle of the crack becomes equal to the applied stress. To that end, an appropriate balance between sufficiently high fiber bridging stress-transfer capacity and sufficiently low matrix toughness must exist.

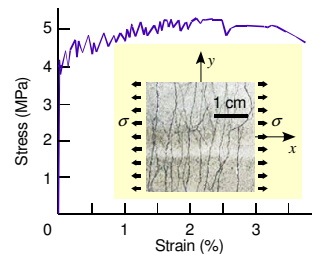


Figure 1: Multiple cracking in a cementitious composite

- (b) The ‘*further cracking criterion*’ requires that the matrix cracking strength (far field stress at which a throughout matrix crack forms) is lower than the maximum bridging stress (maximum stress that bridging fibers can transfer across crack). Consequently, additional parallel cracks can form under further loading.

By means of upscaling, the bridging relation can be linked to micromechanical parameters of fiber, matrix and their interface (Li [3]). The matrix cracking strength depends on the size of initial flaws and matrix fracture toughness (e.g. Wu and Li [4]). With help of these relations, the material composition can be optimized to satisfy the above criteria as well as workability requirements. Initially, researchers mostly focused on the optimization of the fiber-matrix-interface system so as to improve the bridging relationship. In a recent work, Wang and Li [5] experimentally investigated the possibility of tailoring the matrix cracking strength through controlling the flaw size distribution. The study showed that a robust multiple-cracking behavior can be achieved by introducing artificial flaws in the form of low-strength particles of appropriate size.

In the present paper, we attempt to formulate a theoretical model, which can reproduce/predict the phenomena of multiple cracking under uniaxial tension, with a special attention to capture the effect of the initial flaw size distribution. The model employs an approach, which is in principle similar to that used by Wu and Li [4]. In addition, the proposed model uses realistic information on flaw shape and sizes obtained from image analysis of composite sections and accounts for scatter of fiber volume fraction among different crack planes.

2 THE PROCESS OF MULTIPLE CRACKING

Let us consider a specimen of ECC material, which is exposed to uniform uniaxial tension σ in direction x . The specimen’s behavior is initially linearly elastic until the applied load attains the level of the first crack strength σ_{fc} , at which matrix cracking starts. Due to low matrix toughness, the crack propagates almost instantaneously through the specimen in the direction perpendicular to loading. However, the crack is bridged by fibers, which ensure that the crack maintains a flat shape with opening displacement almost uniform along its area. Furthermore, the crack exhibits a hardening response, i.e., increased load is needed to further open the crack. Note that formation of ‘flat’ cracks and hardening crack response are direct consequences of satisfying Criterion (a). If additional loading is applied to the specimen, it causes formation of another matrix crack [Criterion (b)]. The whole scenario then repeats, resulting in a set of throughout cracks distributed along the loading direction x , as seen in the inset of Figure 1.

If the specimen is tested under displacement control, the initial linearly elastic response is followed by numerous fluctuations of the measured stress, as it is obvious in the graph in Figure 1. This overall behavior results from the process of multiple cracking. Each local peak corresponds to formation of a new matrix crack. The stress drop corresponds to the reduction of energy stored in the composite when the new crack forms. The gradual stress increase is associated with further deformation of the specimen, which consists of elastic stretching of the intact composite between cracks and opening/reopening of all multiple cracks.

3 MODEL OF MULTIPLE CRACKING

3.1 Cracking criterion

Most analytical models to date (e.g. Li and Wu [6]) idealized initial flaws as penny-shaped cracks bridged by fibers. The cracking criterion was then formulated by comparing the stress intensity factor (or J-integral) due to the applied load, reduced by the effect of bridging, to the fracture resistance of matrix. However, direct observations of sliced composite specimens reveal that most flaws occur in the shape of round cavities – bubbles of entrapped air (Figure 2). Should the flaws be idealized as spherical cavities, they would be free of stress singularity and the stress

concentration factor around each flaw would be independent of its size. This, in turn, would imply that matrix cracking strength is independent of the flaw size, which contradicts experimental observations. Furthermore, Wang and Li [5] observed sharp cracks propagating from the round flaws. Thus, we model the flaws as round cavities with wing cracks embedded in infinite domain (Figure 2). The

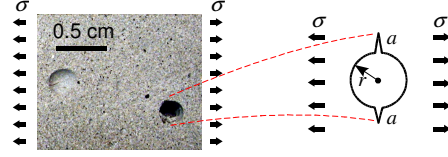


Figure 2: Intrinsic flaws in a cementitious composite

The stress intensity factor (SIF) of such a flaw rapidly increases from 0 (for a round cavity only) to the value of SIF of a penny-shaped crack as the ratio of the wing crack length a to the cavity radius r increases. Therefore we formulate the cracking criterion in the following form:

$${}^{(i)}\sigma_{cr} = K'_m / \sqrt{\pi} {}^{(i)}r, \quad (1)$$

where $K'_m = K_m/F$, K_m is the matrix fracture toughness, F is a factor accounting for a flaw shape (3-D, presence of wing cracks, etc.), and ${}^{(i)}\sigma_{cr}$ is the cracking strength associated with crack initiated at i -th flaw with radius ${}^{(i)}r$. The value of K'_m is calibrated from the first cracking strength σ_{fc} measured in a direct tension test and the radius of the largest flaw observed on the first crack plane; then it can be considered as a material characteristic of a given matrix containing flaws of similar shape.

3.2 Bridging stress

The effect of fiber bridging is represented by bridging stress, which is defined as the sum of forces carried by all fibers spanning a crack, divided by the crack area. Employing the micromechanical model presented by Li [3], for *opening* cracks the bridging stress can be related to the crack opening displacement (COD) δ through the following relationship:

$$\sigma^b(\delta) = \sigma_0 \left[2(\delta/\delta_0)^{1/2} - \delta/\delta_0 \right], \quad (2)$$

where σ_0 is the maximum stress, that can be carried by fiber bridging and δ_0 is the COD at the maximum bridging stress:

$$\sigma_0 = \frac{g\tau V_f L_f}{2d_f}, \quad \delta_0 = \tau L_f^2 \left\{ E_f d_f \left[1 + \frac{V_f E_f}{(1-V_f) E_m} \right] \right\}^{-1}. \quad (3)$$

Here E_f , L_f , and d_f are fiber Young's modulus, length, and diameter, respectively, τ is the fiber-matrix interface frictional bond strength, g is the snubbing factor, E_m is matrix Young's modulus, and V_f is the fiber volume fraction. Note that from Equation (2) we can express δ as a function of σ^b and denote it as:

$$\delta^l(\sigma^b) = \frac{1}{\sigma_0^2} \left[\delta_0 \sigma_0 (2\sigma_0 - \sigma^b) - 2\sqrt{\delta_0^2 \sigma_0^3 (\sigma_0 - \sigma^b)} \right]. \quad (4)$$

For cracks that undergo *unloading* from stress σ^* and COD δ^* or *reloading*, we consider the elastic behavior: the COD decreases linearly with slope k , i.e.:

$$\delta^u(\sigma^b) = \delta^* - \frac{\sigma^* - \sigma^b}{k}, \quad (5)$$

where k corresponds to the elastic stiffness of the bare portions of bridging fibers.

3.3 Overall strain

Assuming that each crack in the uniformly loaded specimen has a uniform width along its area, a homogenization procedure allows us to express the overall strain in the loading direction as:

$$\varepsilon = \varepsilon^{int} + \sum_{i=1}^p \frac{{}^{(i)}\delta}{l}, \quad (6)$$

where ε^{int} is the strain of an intact composite between cracks, ${}^{(i)}\delta$ is the opening displacement of the i -th crack, and p is the number of cracks within gauge length l .

3.4 Overall stress

Assuming that all cracks in the uniformly stressed specimen are perpendicular to the loading direction and cut throughout the specimen with a uniform COD, the loading stress σ must be equilibrated by the bridging stress σ^b on each crack (i.e., the stresses have to be equal). The overall (average) stress is then also equal to the loading stress.

3.5 The relationship between overall stress and overall strain – stress fluctuations

The relationship between overall stress and strain is derived for a composite specimen undergoing multiple cracking in a displacement-controlled uniaxial tensile test. Let us consider the state when there have been $(p-1)$ cracks in the specimen, and the p -th crack just forms at stress ${}^{(p)}\sigma = {}^{(p)}\sigma_{cr}$ and overall strain ${}^{(p)}\varepsilon$. The crack forms and opens instantaneously, while the strain ${}^{(p)}\varepsilon$ remains constant (the test is displacement controlled). While the new p -th crack opens, the ‘older’ $(p-1)$ cracks are unloaded. At the same time, the applied stress and the bridging stresses of all cracks must remain in equilibrium (equal). Thus, the acting stress must drop to level ${}^{(p)}\tilde{\sigma}$, which is obtained by solving eqn (6), in which we have substituted eqn (5) for unloaded cracks, eqn (4) for the new opening crack, and Hooke’s law for the intact composite:

$${}^{(p)}\varepsilon = \frac{{}^{(p)}\tilde{\sigma}}{E_c} + \sum_{i=1}^{p-1} \frac{{}^{(i)}\delta^u({}^{(p)}\tilde{\sigma})}{l} + \frac{{}^{(p)}\delta^l({}^{(p)}\tilde{\sigma})}{l}, \quad (7)$$

where E_c is the overall elastic modulus of the specimen prior to cracking. If the specimen is exposed to further extension, the above equation can be used to obtain the relation between overall strain and stress in the form of:

$$\varepsilon(\sigma) = \frac{\sigma}{E_c} + \sum_{i=1}^{p-1} \frac{{}^{(i)}\delta^u(\sigma)}{l} + \frac{{}^{(p)}\delta^l(\sigma)}{l} \quad (8)$$

until the load rebounds to the level of ${}^{(p)}\sigma$, since until this moment, the ‘older’ $(p-1)$ cracks respond to reloading along the same path as to unloading. After the load exceeds the level of ${}^{(p)}\sigma$, all the cracks open according to eqn (4). Thus,

$$\varepsilon(\sigma) = \frac{\sigma}{E_c} + \sum_{i=1}^p \frac{{}^{(i)}\delta^l(\sigma)}{l}, \quad (9)$$

which can be used until the next crack forms upon satisfaction of the criterion ${}^{(p+1)}\sigma = {}^{(p+1)}\sigma_{cr}$.

3.6 Stochastic variables

Microscopic observations show that the intrinsic matrix flaws (air bubbles) have various sizes ranging from tenths of mm to several mm. Also, the artificial flaws usually do not have a perfectly

round shape and uniform size (although the scatter is less than that of the natural ones). Consequently, the flaw size is treated as a random variable within a specimen volume.

Equations (3), which define the maximum bridging stress and COD at this stress, were derived by spatial averaging of fiber bridging forces over a crack plane. The fiber-scale parameters E_f , L_f , d_f , τ , and g can be then interpreted as averaged values of all fibers bridging a crack plane and consequently they can be assumed to be the same for all cracks. On the contrary, the fiber volume fraction V_f in reality varies between individual crack planes (namely due to material processing in fresh state). Consequently V_f is also treated as a random variable. This implies that different values of δ_0 and σ_0 are used for each crack.

4 DETERMINATION OF STATISTICAL CHARACTERISTICS

The statistical distribution of flaw size is obtained from 3-D reconstruction of a composite microstructure. To this end, images of planar sections of a composite specimen are first processed by image analysis program: intersection area of each flaw is determined and the radius of a circle with equivalent area is calculated. Note that these are not the desired radii of flaws, since the sections almost never cut through the flaw center. Consequently, a 3-D model of the specimen is constructed, in which flaws are represented by spheres with variable radius randomly located in the specimen volume. The model is intersected by the same number of planes as the physical specimen and radii of the flaw intersections are calculated. The statistical distribution of the flaw radii used to construct the 3-D model is then iteratively adjusted so as to obtain a close matching of the model sectional data to those of the real specimen. It is noted that this crude method will be in future work replaced by a more sophisticated optimization-based approach (Cule and Torquato [7]).

The statistical distribution of fiber volume fraction along the loaded direction of a composite specimen can be also obtained through image analysis of planar sections. The procedure is simpler than in the case of intrinsic flaws, since V_f can be estimated from the number of intersected fibers (Li [3]).

5 NUMERICAL SIMULATION OF MULTIPLE CRACKING PROCESS

The simulation of the multiple cracking process is based on the 3-D reconstruction of a specimen microstructure discussed in section 4. Flaws are sorted in a descending order with respect to their size and fracture criterion (1) is used to calculate the overall stress at which each flaw is activated to form a throughout matrix crack. Consequently, each crack plane is assigned a value of V_f , which is generated as a pseudorandom number with appropriate distribution (see section 4). The relations provided in section 3 are then used to calculate the overall stress-strain curve for increasing number of cracks. The process is terminated when the COD of any of the existing cracks attains the value of δ_0 corresponding to its V_f ; when this condition is satisfied, the hardening capacity of the crack has been exhausted and the specimen fails.

The above procedure has been applied to simulate the behavior of ECC materials tested by Wang and Li [5]. Composite denoted as Mix 1 contained only natural flaws, while in Mix 2 the flaw size was controlled by addition of 7% by volume of weak particles. Both materials contained the same amount of short PVA fibers (2% by volume). Since sectional images were available only for Mix 1, the method described in section 4 was used to determine flaw size distribution only for this material. The microstructure of Mix 2 was obtained by adding 7% by volume of extra flaws (representing the weak particles) to Mix 1. The weak particles' radii were assumed to follow a normal distribution with mean value of 1.75 mm and standard deviation of 0.2. As intersected fibers could not be counted from the available images, V_f was characterized by normal distribution with mean value of 0.02 and the standard deviation was assumed to be 0.002 for both materials.

All remaining parameters were the same for both materials. The value of $K'_m = 14 \text{ MPa}\cdot\text{mm}^{0.5}$ was calibrated from Mix 1.

Figure 3 compares the computed responses of Mix 1 and Mix 2. The results match fairly well the experimental results reported by Wang and Li [5]. In particular, the analysis captures the improvement of the composite ductility that can be achieved by controlling the flaw size.

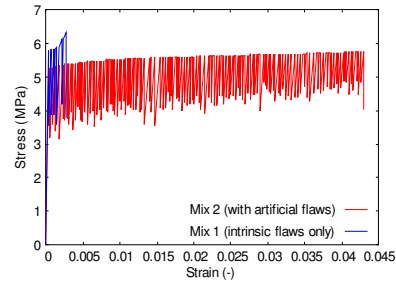


Figure 3: Calculated stress-strain curves of ECC materials

6 CONCLUDING REMARKS

The presented approach allows prediction of the overall stress-strain curve of fiber reinforced cementitious composites exhibiting multiple cracking. Though it was not discussed in the paper, the model also provides information on actual width of the distributed multiple cracks at given overall deformation, which may be important when the material is used for crack width control. Since the model accepts micromechanical parameters of the fiber-matrix-interface system and stochastic characterization of the material microstructure as the input, it can be used as a tool for optimization of material composition.

Figure 3: Calculated stress-strain curves of ECC materials

7 REFERENCES

- [1] Li, V.C., Reflections on the research and development of Engineered Cementitious Composites (ECC), in Proc. of the JCI International Workshop on Ductile Fiber Reinforced Cementitious Composites (DFRCC) – Application and Evaluation, 1-21, 2002.
- [2] Leung, C.K.Y., Design criteria for pseudoductile fiber-reinforced composites, *Journal of Engineering Mechanics*, 122 (1), 10-18, 1996.
- [3] Li, V.C., Post-crack scaling relations for fiber-reinforced cementitious composites, *ASCE Journal of Materials in Civil Engineering*, 4 (1), 41-57, 1992.
- [4] Wu, H.C. and Li, V.C., Stochastic process of multiple cracking in discontinuous random fiber reinforced brittle matrix composites, *International Journal of Damage Mechanics*, 4, 83-102, 1995.
- [5] Wang, S. and Li, V.C., Tailoring of pre-existing flaws in ECC matrix for saturated strain hardening, in *Fracture Mechanics of Concrete Structures* (V.C. Li, C.K.Y. Leung, K. J. Willam, S.L. Billington eds.), 1005-1012, 2004.
- [6] Li, V.C. and Wu, H.C., Conditions for pseudo strain-hardening in fiber reinforced brittle matrix composites, *Journal of Applied Mechanics Review*, 45 (8), 390-398, 1992.
- [7] Cule, D. and Torquato, S., Generating random media from limited microstructural information via stochastic optimization, *Journal of Applied Physics*, 86 (6), 3428-3437, 1999.

8 ACKNOWLEDGEMENT

The authors would like to thank to Mr. Shuxin Wang from the University of Michigan for providing his experimental data and specimen images and for inspiring discussions. The research presented in this paper was supported by grant of the Czech Science Foundation GACR 106/02/0678 and Contract of the Czech Ministry of Education 210000003.